

Temperature-dependent electronic structure and magnetic stability of thin ferromagnetic films

W. Nolting^a and C. Santos^a

^aLehrstuhl Festkörpertheorie, Institut für Physik, Humboldt-Universität zu Berlin, Invalidenstr. 110, 10115 Berlin, Germany

We study correlation effects and temperature dependencies in the electronic structure of thin ferromagnetic local-moment films. In a first step the Kondo-lattice model is investigated as a candidate for a proper representation of local-moment ferromagnets. Magnetic and electronic key-quantities as the Curie-temperature and the quasiparticle density of states are derived with previously tested many-body procedures. It is shown that the magnetic properties can be interpreted exclusively in terms of the temperature-dependent electronic quasiparticle structure. An extended RKKY theory leads to effective Heisenberg exchange integrals, which turn out to be functionals of the conduction electron selfenergy, getting therewith a remarkable temperature and band occupation dependence.

In a second step the model studies are combined with tight binding-LMTO bandstructure calculations in order to get for real ferromagnetic films quasiparticle densities of states and quasiparticle bandstructures. The proposed method avoids the double-counting of relevant interactions and takes into account the correct symmetry of the atomic orbitals. Special results are given for thin ferromagnetic EuO (100) films. The Curie temperature T_C of the EuO film turns out to be strongly thickness-dependent, starting from a very low value ($\simeq 15K$) for the monolayer and reaching the bulk value at about 30 layers. For a 20-layer film we predict the existence of a surface state, the temperature-behaviour of which can lead to a surface halfmetal-insulator transition.

1. Introduction

All key-quantities of ferromagnetism (Curie-temperature T_C , magnetic moment μ , magnetization $M(T)$, susceptibility χ , ...) are in the last analysis consequences of the electronic structure of the respective magnetic material. To understand ferromagnetism therefore means to understand the temperature-dependent electronic structure. Our method, which we use to get reliable information in this respect, consists of three steps. First we choose a proper theoretical model, defined by its Hamiltonian

$$H = H_0 + H_I \quad (1)$$

more strictly by the interaction part H_I which shall incorporate all those interactions which are considered as relevant for the physical problem under study. The single-particle part, on the other hand, shall cover, besides the usual kinetic energy and the periodic lattice potential, the influences of all the other interactions which are not directly accounted for by H_I . By definition they

are not decisive for magnetism and the characteristic temperature-dependent electronic structure, but nevertheless, they may determine the rough structure of the energy spectrum being therefore non-negligible if our study aims at a more or less quantitative electronic structure description. We therefore perform in the second step a first principles bandstructure calculation on the basis of density functional theory (DFT) and use the results as single-particle energies in H_0 . So we guarantee that all the other interactions show up in H_0 in an averaged but fairly realistic manner. However, one has carefully to avoid a double counting of just the relevant interactions, once explicitly in H_I and then once more implicitly in the renormalized single-particle energies. How to circumvent this serious and well-known double counting problem shall be explained for the actual problem at a later stage of this paper.

As a third step a many-body formalism is used for (1) to work out how the effective single-particle energies change under the rele-

vant interactions H_I into a temperature- and concentration-dependent selfenergy $\Sigma_{\mathbf{k}\sigma}(E)$ from which we derive the quasiparticle bandstructure (Q-BS). The latter directly corresponds to the data of an angle- and spin-resolved photoemission experiment.

We proceed in the following exactly along the line given by the just-developed concept. To do the first step, the fixing of a proper theoretical model, requires of course above all to agree upon which type of magnetic material shall be studied. We concentrate ourselves in this paper on so-called local-moment systems, i. e. on materials, the magnetic properties of which are due to strictly localized moments, while the conductivity properties are provoked by extended band states. Typical examples are magnetic insulators such as EuO, EuS [1] and magnetic metals as Gd [2], which all have strictly localized moments because of the half-filled $4f$ shell of the rare earth ion (Eu^{2+} , Gd^{3+}). Many striking features of these materials can be traced back to an intimate correlation between the localized magnetic moments and the extended band states. The same interaction is considered responsible for the properties of the intensively investigated diluted magnetic semiconductors like $\text{Ga}_{1-x}\text{Mn}_x\text{As}$. The ion creates simultaneously a localized $S = 5/2$ moment and an itinerant hole in the GaAs valence band [3], the interaction of which leads to ferromagnetism already for very low concentrations x . Another burning issue in this respect are the colossal magnetoresistance (CMR) materials [4] such as $\text{La}_{1-x}(\text{Ca}, \text{Sr})_x\text{MnO}_3$ which exhibit a rich magnetic phase diagram as function of x . For $0.2 \leq x \leq 0.4$ the original insulating antiferromagnetic parent compound LaMnO_3 becomes a ferromagnetic metal. This is ascribed to a homogeneous valence mixing ($\text{Mn}_{1-x}^{3+}\text{Mn}_x^{4+}$). The three $5d - t_{2g}$ electrons in Mn^{3+} form a localized $S = 3/2$ moment while the additional $5d - e_g$ electron is itinerant. Again the local moment-itinerant electron correlation is likely responsible for many typical features of the CMR materials.

2. Kondo Lattice Model (KLM)

A model which provides an at least qualitatively correct insight into the physics of the local-moment systems is the Kondo-lattice model, which shall now be investigated in detail.

2.1. Model Hamiltonian, Exact Limiting Case

The KLM describes interacting local moments (spins \mathbf{S}_i) and itinerant electrons in a nondegenerate s -band:

$$H = \sum_{ij\sigma} T_{ij} c_{i\sigma}^\dagger c_{j\sigma} - J \sum_j \boldsymbol{\sigma}_j \cdot \mathbf{S}_j \quad (2)$$

$c_{i\sigma}^\dagger (c_{i\sigma})$ creates (annihilates) a band electron with spin σ ($\sigma = \uparrow, \downarrow$) at the lattice site \mathbf{R}_i . T_{ij} are the hopping integrals. The "a priori" uncorrelated electrons are exchange coupled to the local moments, where this coupling is considered an on-site interaction of the electron spin $\boldsymbol{\sigma}_i$ and the localized spin \mathbf{S}_i . J is the coupling constant. Using second quantization for the electron spin operator the interaction term reads:

$$H_I = -\frac{J}{2} \sum_j \left(S_j^z (n_{j\uparrow} - n_{j\downarrow}) + S_j^+ c_{j\downarrow}^\dagger c_{j\uparrow} + S_j^- c_{j\uparrow}^\dagger c_{j\downarrow} \right) \quad (3)$$

($n_{j\sigma} = c_{j\sigma}^\dagger c_{j\sigma}$). The first term represents an "Ising-type" interaction while the two others refer to spin exchange processes. The latter give rise to some of the most typical KLM properties. Spin exchange may happen in three different elementary processes: magnon emission by a \downarrow electron, magnon absorption by a \uparrow electron and formation of a quasiparticle known as "magnetic polaron". The quasiparticle can be understood as a propagating electron dressed by a virtual cloud of magnons corresponding to a polarization of the immediate localized spin neighbourhood.

The sophisticated many-body problem provoked by the KLM-Hamiltonian (2) can in general not be solved exactly. Luckily there exists a non-trivial limiting case which is rigorously treatable exhibiting all the just-mentioned important elementary exchange processes. It is the situation of a ferromagnetically saturated semiconductor (EuO at $T = 0$), i. e. a single electron in

an otherwise empty conduction band coupled to a saturated moment system. In this case the \uparrow spectrum is extremely simple because the \uparrow electron has no chance to exchange its spin with the parallel aligned spin system. Only the Ising-type interaction in (3) takes care for a rigid shift of the spectrum of $-\frac{1}{2}JS$. The quasiparticle density of states (Q-DOS) is identical to the free Bloch density of states (B-DOS), $\rho_{\uparrow}(E) = \rho_0(E + \frac{1}{2}JS)$, expect for the trivial shift of $-\frac{1}{2}JS$. On the contrary, real correlation effects make the \downarrow spectrum highly non-trivial. Fig. 1 shows the \downarrow -Q-BS as density plot of the respective spectral den-

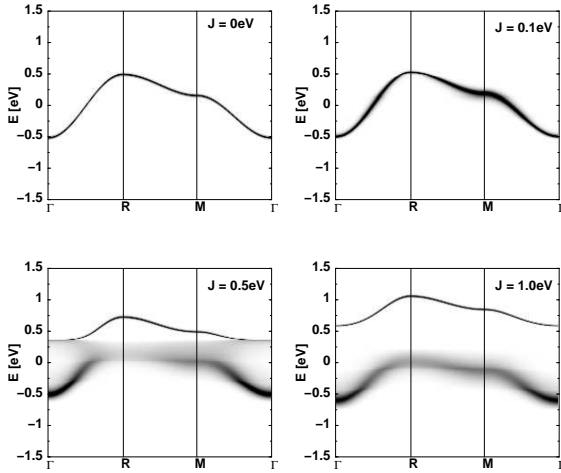


Figure 1. Down-spin quasiparticle bandstructure of a ferromagnetically saturated semiconductor along several symmetry directions for different exchange couplings J . The degree of blackening in the bandstructure is a measure of the magnitude of the spectral density. Parameters: $S = 1/2$, $W = 1\text{eV}$, s.c. lattice. $J = 0$ means the interaction-free Bloch-dispersion.

sity. The degree of blackening is a measure for the height of the quasiparticle peak. Rather moderate effective exchange couplings JS/W are already sufficient to split the energy dispersion into

two branches. The sharp high-energy one belongs to the magnetic polaron, which has in this case even an infinite lifetime ("bound state"). The low-energy branch is stronger washed out. It is due to magnon emission by the \downarrow electron which thereby reverses its spin. The magnon can carry away any wave vector from the first Brillouin zone. The spectrum ("scattering spectrum") is therefore in general rather broad. Because of the spinflip it extends over just that energy region where $\rho_{\uparrow}(E) \neq 0$. Surprisingly, however, the broad scattering part is often bunched together to a rather prominent quasiparticle dispersion. The splitting of the original Bloch dispersion into two quasiparticle branches is a typical correlation effect, by no means reproducible by a single-particle theory.

2.2. Many-Body Evaluation

For the general case (finite temperature, finite band occupations) the many-body problem of the KLM can only be solved approximately. A common feature of many approaches is the following structure of the conduction electron selfenergy [5,6]

$$\Sigma_{\mathbf{k}\sigma}(E) = -\frac{1}{2}Jz_{\sigma}\langle S^z \rangle + J^2 D_{\mathbf{k}\sigma}(E) \quad (4)$$

If restricting to the first term, only, one has the mean-field approach to the KLM, which is correct for sufficiently weak couplings J . This part is mainly due to the Ising-interaction in (3). Without the second term, it would lead to a spin-polarized splitting of the conduction band ($z_{\sigma} = \delta_{\sigma\uparrow} - \delta_{\sigma\downarrow}$). The more complicated second part contains the spin exchange processes and the polaron formation. In a previous paper [5] we have proposed a moment conserving decoupling approach (MCDA) for a set of properly defined Green functions that correctly reproduces the exactly solvable limiting cases of the KLM. For details of the derivation the reader is referred to ref. [5]. The MCDA demonstrates that the self-energy carries a distinct temperature-dependence which is brought into play by two different types of spin correlations. There are mixed correlations such as $\langle S_i^z n_{i\sigma} \rangle$, $\langle S_i^+ c_{i\downarrow}^{\dagger} c_{i\uparrow} \rangle$, ... built up by combinations of localized-spin and itinerant-electron

operators. Luckily all these correlations can be expressed via the spectral theorem by one of the Green functions involved in the MCDA. There is no need for further approximations. The second type of correlations are pure local-moment correlations: $\langle S_i^z \rangle$, $\langle S_i^\pm S_i^\mp \rangle$, $\langle (S_i^z)^3 \rangle$, ... which need a special treatment.

We use a "modified" RKKY (M-RKKY) theory [5,7] which exploits a mapping of the interband exchange (3) to an effective Heisenberg model,

$$H_f = - \sum_{ij} J_{ij} \mathbf{S}_i \cdot \mathbf{S}_j, \quad (5)$$

by averaging out the conduction electron degrees of freedom:

$$H_I \longrightarrow \langle H_I \rangle^{(c)} = -J \sum_j \mathbf{S}_j \langle \boldsymbol{\sigma}_j \rangle^{(c)} \longrightarrow H_f \quad (6)$$

$\langle \dots \rangle^{(c)}$ means averaging in the subspace of the conduction electrons. Details of the applied Green-function procedure can be found in refs. [5, 7]. The result are effective exchange integrals J_{ij} in (5):

$$J_{ij} = \frac{J^2}{4\pi N^2} \sum_{\mathbf{k}, \mathbf{q}, \sigma} e^{i\mathbf{q} \cdot (\mathbf{R}_i - \mathbf{R}_j)} \int_{-\infty}^{+\infty} dE f_{-}(E) \times \quad (7)$$

$$\text{Im} \left[(E - \varepsilon_{\mathbf{k}} + i0^+) (E - \varepsilon_{\mathbf{k}+\mathbf{q}} - \Sigma_{\mathbf{k}+\mathbf{q}\sigma}(E)) \right]^{-1}$$

$f_{-}(E)$ is the Fermi function. Most important is the appearance of the conduction electron selfenergy on the right hand side. Neglecting Σ_{σ} leads to the "conventional" RKKY formula with $J_{ij} \sim J^2$, as a result of second order perturbation theory. By Σ_{σ} higher order conduction electron spin polarization terms enter the M-RKKY as well as a distinct temperature-dependence. With (5) and (7) we calculate the above-mentioned local moment correlations, applying a standard Tyablikow-approximation to the Heisenberg model [7]. Together with (4) a closed system of equations is built up which can be solved self-consistently for all electronic or magnetic KLM-properties, we are interested in. Results are presented in the next Section.

2.3. KLM-Bulk Properties

Fig. 2 shows the Q-BS and the Q-DOS for a model system on a s.c. lattice with $S = 7/2$, a moderate exchange coupling $J = 0.2\text{eV}$ and a band occupation $n = 0.2$. For this parameter constellation the self-consistently calculated Curie temperature amounts to 238K . At low temperatures ($T = 37\text{K}$) the local moments are

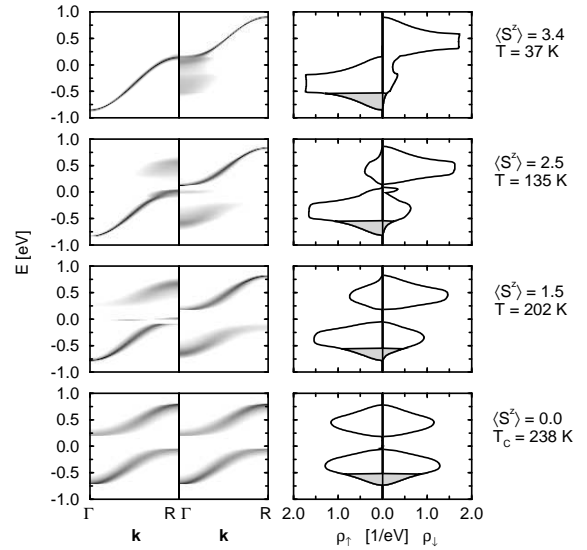


Figure 2. Quasiparticle bandstructure as a function of wave-vector (left column) and quasiparticle density of states as a function of energy (right column) for four different temperatures calculated within the MCDA [5]. Parameters: $S = 7/2$, $W = 1\text{eV}$, $J = 0.2\text{eV}$, $n = 0.2$, s.c. lattice.

almost saturated, and therefore the \uparrow -dispersion and the Q-DOS ρ_{\uparrow} are practically identical to the respective "free" functions according to the limiting case discussed in Sect. 2.2. The \downarrow spectrum, however, is more complicated. In the Q-BS the scattering states are clearly visible near the Γ point, while near the R point the magnetic polaron states dominate. One recognizes

that $\rho_{\downarrow}(E)$ has a low-energy tail, which covers exactly the same energy region as $\rho_{\uparrow}(E)$. This tail consists of scattering states (magnon emission!) which belong to spin-flip excitations of the \downarrow electron. Such processes are of course possible only when there are \uparrow -states within reach. That explains the coincidence of the low-energy tail of $\rho_{\downarrow}(E)$ with $\rho_{\uparrow}(E)$ at low temperatures.

With increasing temperature, decreasing moment magnetization $\langle S^z \rangle$, more and more magnons are created which can be absorbed by the \uparrow electron. Consequently, scattering states (magnon absorption!) appear in the \uparrow spectrum, too. Q-BS as well as Q-DOS for \uparrow and \downarrow continuously approach each other with increasing T , at T_C the spin asymmetry is removed. However, a correlation-caused splitting of the energy dispersion and a splitting of the conduction band into two quasiparticle subbands remains which should be observable in a respective photoemission experiment.

The most important entity of ferromagnetism is the Curie temperature T_C . So it is worthwhile to have a look on its dependence on model parameters like band occupation n and exchange coupling J (Fig. 3). Low electron (hole) densities appear to be convenient for a ferromagnetic ordering of the local moments, where the ferromagnetic region increases with increasing J . Around half-filling ($n = 1$) ferromagnetism is excluded. Even more striking and substantially deviating from the conventional RKKY picture is the J -dependence of T_C (Fig. 3b). Except for very low electron densities n there exist a lower and an upper critical J_c . Finite Curie temperatures appear only between these two limits, which in addition are approaching each other with increasing n . This is a new feature which goes far beyond textbook-RKKY and has delicate consequences for the application of the KLM to strongly coupled ferromagnetic local moment systems like $\text{Ga}_{1-x}\text{Mn}_x\text{As}$ and $\text{La}_{1-x}(\text{Ca}, \text{Sr})_x\text{MnO}_3$. On the other hand, the results in Fig. 3b do not exclude a reappearance of ferromagnetism for still stronger J . This could not be checked up to now.

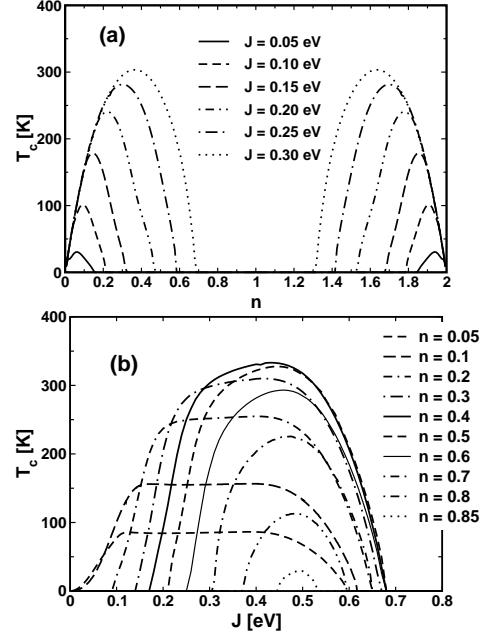


Figure 3. Curie temperature as function of (a) the band occupation n , (b) the interband exchange coupling J for various (a) J , (b) n , calculated by use of the "modified" RKKY [7]. Other parameters as in Fig. 2.

3. Ferromagnetic Local-Moment Films

According to the general scheme annotated in the Introduction we are now going to combine the preceding model study with a first-principles bandstructure calculation in order to investigate the electronic structure of a real ferromagnetic material. In particular, we want to present results for thin ferromagnetic EuO films. Some preparations are still necessary.

3.1. Model Films

We consider a film as a piece of solid consisting of n monolayers parallel to two surfaces. The monolayers are numbered by Greek letters ($\alpha, \beta, \dots = 1, 2, \dots, n$). We assume translational symmetry within the two-dimensional surfaces, so that the film can be described as a two-

dimensional Bravais lattice (\mathbf{R}_i) with an n -atomic basis (\mathbf{r}_α):

$$\mathbf{R}_{i\alpha} = \mathbf{R}_i + \mathbf{r}_\alpha \quad (8)$$

The influence of the surface consists in the forbidden electron hopping in the third space-direction and a possibly modified hopping near the surface, which may give rise to the appearance of surface states.

Because of the two-dimensional translational symmetry the thermodynamic average of any site-dependent operator $O_{i\alpha}$ is independent of the Bravais-index i , but may retain a layer-dependence $\langle O_{i\alpha} \rangle = \langle O_\alpha \rangle$. That holds, in particular, for many-body terms like Green functions, spectral densities and Q-DOS. Fourier-transforms use wave-vectors from the two-dimensional Brillouin zone of the surface, e.g.:

$$\Sigma_{\mathbf{k}\sigma}^{\alpha\beta}(E) = \frac{1}{N} \sum_{ij} \Sigma_{ij}^{\alpha\beta}(E) e^{-i\mathbf{k} \cdot (\mathbf{R}_i - \mathbf{R}_j)} \quad (9)$$

The many-body concepts, developed for the bulk (Sect. 2), remain, however, exactly the same for the film. The only difference is that the central equations of the theory now appear in matrix form. That complicates a little bit the numerical evaluation.

The interesting question is whether or not the correlation effects, worked out for the bulk-KLM in Sect. 2, are decisively influenced by the reduced symmetry of a thin film. As an example we present in Fig. 4 the local Q-DOS ρ_σ^α of a semiconducting 20-layer s.c.-film for three different exchange couplings J and various temperatures [8]. There is a clearly visible layer dependence of ρ_σ^α . However, the physical interpretation is exactly the same as for the bulk (Fig. 2). All quasiparticle features remain valid and determine the striking temperature dependence of the Q-DOS, in film structures, too. A new feature is the possible appearance of surface states as a consequence of the modified hopping near and within the surface. That will be inspected in Sect. 3.3 with respect to a EuO (100)-film.

3.2. Multiband Kondo Lattice Model

To apply our model study to a ferromagnetic EuO (100) film we have first to remove some

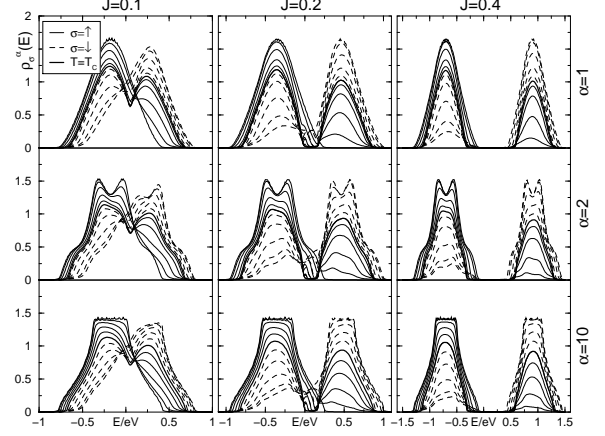


Figure 4. Local quasiparticle density of states of the first ($\alpha = 1, 20$), second ($\alpha = 2, 19$), and center ($\alpha = 10, 11$) layer of a 20-layer s.c.- (100) film for different interband exchange couplings J and different temperatures $T/T_C = 0, 0.4, 0.7, 0.9, 0.98, 1$. The bold lines are for $T = T_C$, the outermost curves belong to $T = 0$ (full lines: up-spin, broken lines: down-spin). Ferromagnetic semiconductor: $n = 0$.

model simplifications. The (empty) conduction bands of EuO have $5d$ character. So we have to replace the previous assumption of a non-degenerate s -band accordingly. Instead of (1) we write

$$H = H_d + H_f + H_I \quad (10)$$

H_d refers to the conduction bands:

$$H_d = \sum_{ij\alpha\beta\sigma} \sum_{mm'} T_{ij\alpha\beta}^{mm'} c_{i\alpha m\sigma}^\dagger c_{j\beta m'\sigma} \quad (11)$$

m, m' denote different orbitals. $T_{ij\alpha\beta}^{mm'}$ are the hopping integrals ($\mathbf{R}_{i\alpha} \leftrightarrow \mathbf{R}_{j\beta}$) which we take from a first principles bandstructure calculation according to the tight-binding LMTO-ASA program of Anderson [9,10]. The conduction band of the semiconductor EuO is empty at $T = 0$. From the exact limiting case of the KLM (Sect. 2.1) we know that in ferromagnetic saturation the \uparrow spec-

trum is identical to the "free" Bloch-spectrum except for an unimportant rigid shift (Fig. 1, Fig. 2). So we take from the bandstructure calculation the \uparrow spectrum as input for H_d , thereby elegantly circumventing the double counting of the interband exchange. We do not avoid the double counting by "switching off" the relevant interaction part, what appears almost impossible, but by exploiting the exact limiting case, for which this interaction part causes only a rigid shift of the \uparrow spectrum. Remember that the \downarrow spectrum, on the contrary, is influenced by the interband exchange in a drastic manner, even at $T = 0$.

H_f refers to the local moment system (half-filled $4f$ shell of the Eu^{2+} ion), which we describe by an extended Heisenberg Hamiltonian:

$$H_f = - \sum_{ij\alpha\beta} J_{ij}^{\alpha\beta} \mathbf{S}_{i\alpha} \cdot \mathbf{S}_{j\beta} - D_0 \sum_{i\alpha} (S_{i\alpha}^z)^2 \quad (12)$$

The first term is the original Heisenberg Hamiltonian (5), while the second term introduces a symmetry-breaking single-ion anisotropy being necessary to overcome the Mermin-Wagner theorem which excludes a collective magnetic order in the isotropic Heisenberg model for film geometries at finite temperatures [11–13]. Because of the empty conduction bands a self-consistent justification of the EuO-ferromagnetism via an RKKY-type mechanism is not possible. Instead of this we take the experimental values for the exchange integrals between nearest (J_1) and next-nearest neighbours (J_2)[14] ($J_1/k_B = 0.625K$; $J_2/k_B = 0.125K$).

The third term in (10) describes the on-site Coulomb interaction between electrons in different orbitals. By a straightforward consideration[15] one finds an interaction operator in strict generalization of (3):

$$H_I = -J \sum_{i\alpha m} \sigma_{i\alpha m} \cdot \mathbf{S}_{i\alpha} \quad (13)$$

Although the multiorbital situation complicates once more the numerics of the evaluation, nevertheless one can apply the same many-body concepts, successful for the simple KLM (Sect. 3), to the multiband-KLM (10), too. In the next

Section a short list of some typical results is presented.

3.3. EuO (100) Films

Fig. 5 shows the temperature- and layer-dependent magnetization for films of different thickness (from $n = 1$ to $n = 20$ monolayers). For all temperatures and all thicknesses the magnetization $\langle S_\alpha^z \rangle$ increases from the surfaces ($\alpha = 1, n$) to the center layers ($\alpha = \frac{n}{2}$ or $\frac{n+1}{2}$), qualitatively understandable because of the reduced coordination number of the surface atoms. The Curie temperature T_C is obviously strongly thickness-dependent. Starting from about $15K$ for the monolayer T_C steadily increases with n reaching

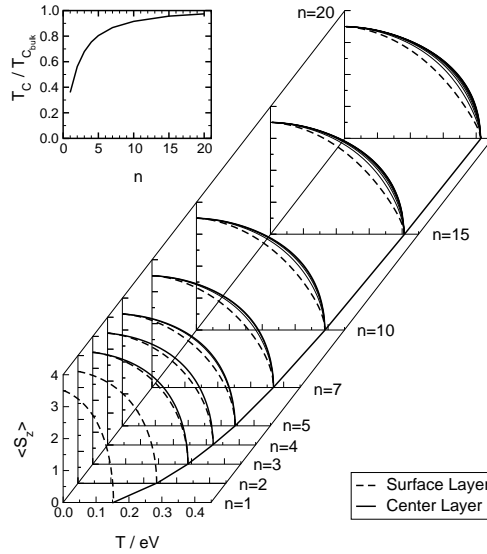


Figure 5. Layer-dependent magnetizations of EuO(100) films as a function of temperature and for various film thicknesses (n = number of monolayers). Parameters $J_1/k_B = 0.125K$, $J_2/k_B = 0.125K$, $D_0/k_B = 0.05K$. Inset: Curie temperature as function of film thickness ($T_C^{\text{Bulk}} = 69.33K$).

the bulk value ($69.33K$ [1]) for $n \approx 30$. The 20-layer film has $T_C = 66.7K$. The $T_C(n)$ curve

in Fig. 5 remarkably resembles that of Gd films [16]. To our knowledge corresponding measurements on EuO films have not been done yet.

The temperature-dependence of the local moment correlations $\langle S_\alpha^z \rangle, \langle S_\alpha^\pm S_\alpha^\mp \rangle, \dots$ transfers via the interband coupling J to the (empty) band states (Fig. 6). The shift of the layer-dependent Q-DOS with temperature is not at all rigid but with strong irregularities, mainly due to the

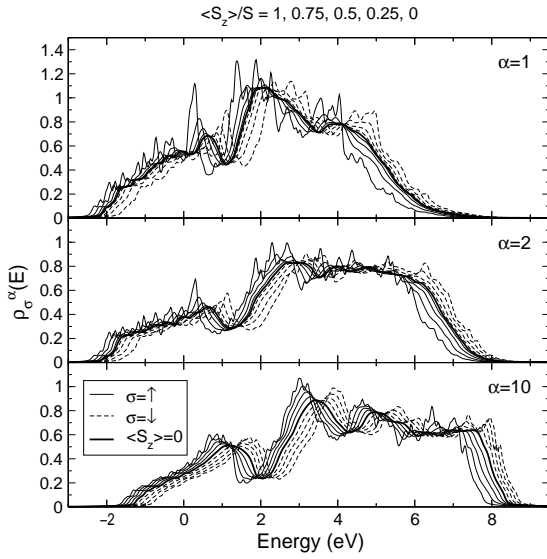


Figure 6. Local quasiparticle densities of states of the empty Eu-5d bands of the first ($\alpha = 1$), second ($\alpha = 2$), and center ($\alpha = 10$) layers of a 20-layer EuO(100) film for different temperatures ($T_C = 66.7K$).

above-discussed spinflip processes. Fig. 6 shows $\rho_\sigma^\alpha(E)$ for a 20-layer film. The lower \uparrow -band edge shifts upon cooling from $T = T_C$ down to $T = 0K$ by some $0.3eV$. This is the famous "red shift", experimentally observed as corresponding shift of the optical absorption edge already some 35 years ago [1].

The Q-DOS of the center layer ($\alpha = 10$) resembles already pretty well the Q-DOS of bulk-EuO [17]. Comparing it with the surface Q-

DOS ($\alpha = 1$) one observes a shift of $\rho_\sigma^{\alpha=1}(E)$ to somewhat lower energies. This is an indication for the appearance of a surface state. A surface state is a state which exists in the so-called forbidden region where no bulk states occur. Typically the spectral weight of a surface state decreases exponentially with increasing distance from the surface. Fig. 7 proves the existence

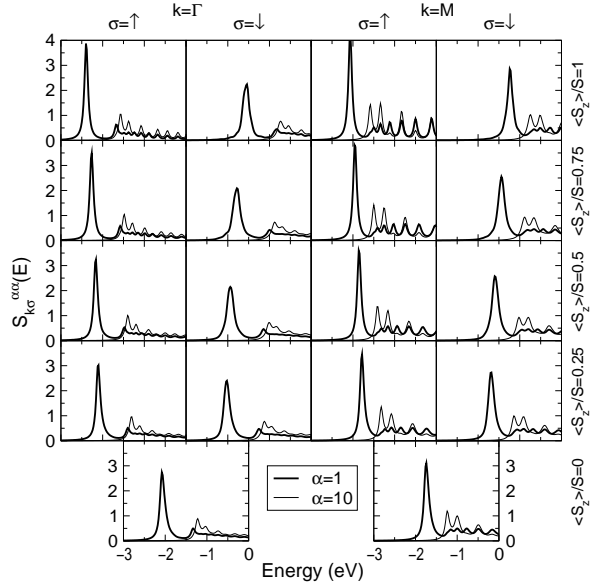


Figure 7. Layer-dependent spectral density of the surface ($\alpha = 1$: thick lines) and the center layer ($\alpha = 10$: thin lines) of a 20-layer EuO(100) film at the Γ point and the M point for $J = 0.25eV$ and for different temperatures ($T_C = 66.7K$).

of the EuO(100) surface state by the spectral density $S_{\mathbf{k}\sigma}^{\alpha}(E)$ of the 20-layer film at $\mathbf{k} = \bar{\Gamma}$ and $\mathbf{k} = \bar{M}$. Below the $\alpha = 10$ spectrum there is for both \mathbf{k} -values a prominent peak of the spectral density for $\alpha = 1$. For $T = 0$ the surface state lies at the $\bar{\Gamma}$ point about $0.8eV$ and the \bar{M} point about $0.45eV$ below the "bulk" ($\alpha = 10$) spectrum. These splittings between surface states and the lower edges of the "bulk" spectrum are practically temperature-independent. The induced spin

splitting of the surface state as well as that of the band states collapses with increasing temperature $T \rightarrow T_C$.

This temperature-behaviour gives rise to an interesting speculation [18]. The gap between the occupied $4f \uparrow$ -states and the empty $5d$ -conduction band states amounts to 1.12eV at $T = T_C$ [1]. The lower edge of the surface band lies 0.8eV below the $5d$ -edge. The red shift of about 0.3eV will further reduce the gap when decreasing the temperature to $T = 0$. The overall gap reduction ($\approx 1.1\text{eV}$) is therefore in the range of the experimental $4f - 5d_{t_{2g}}$ gap of bulk EuO at room temperature. That makes a surface insulator-metal transition in EuO(100) films possible when the film is cooled down to $T \rightarrow 0\text{K}$. Because of the induced exchange splitting of the surface states \uparrow electrons will tunnel from the $4f$ band into the surface band resulting in a halfmetal. Furthermore, the resistivity of the EuO(100) film should be highly reactive to an external magnetic field giving rise to a colossal magnetoresistance effect.

4. Conclusions

With the concrete example of a thin ferromagnetic EuO(100) film we have demonstrated our method of determining magnetic properties of real materials as consequences of the temperature-dependent electronic structure. The method combines the many-body evaluation of a properly chosen theoretical model with a first principles bandstructure calculation in order to get more or less quantitative electronic structure information.

EuO belongs to the so-called local-moment ferromagnets which are reasonably modelled by the Kondo lattice model. We have therefore inspected in detail the properties of this model, first for the bulk and then for film geometries. The results have been brought into contact with a tight-binding linear muffin-tin orbital bandstructure calculation (TB-LMTO). The resulting temperature-dependent electronic structure gave rise to the speculation of a surface insulator-halfmetal transition when cooling the film below T_C . The reason is the Stoner-like temperature

shift of an empty $5d$ surface state (band) with an induced exchange splitting. A colossal magnetoresistance effect may be expected.

Acknowledgements

A great part of this review was fuelled by the PhD. thesis of R. Schiller, submitted at the Humboldt-Universität zu Berlin (Germany). Financial support by the SFB 290 of the "Deutsche Forschungsgemeinschaft" and by the "Volkswagen-Stiftung" is gratefully acknowledged.

REFERENCES

1. P. Wachter, *Handbook of Physics and Chemistry of Rare Earths* Vol. 2, K. A. Gschneidner and L. Eyring (Elsevier, Amsterdam) (1979).
2. M. Donath, P. A. Dowben, and W. Nolting, editors, *Magnetism and Electronic Correlations in Local-Moment Systems; Rare-Earth Elements and Compounds*. World Scientific, Singapore (1998).
3. H. Ohno, *Science* **281**, 951 (1998).
4. A. P. Ramirez, *J. Phys.: Condens. Matter* **9**, 8171 (1997).
5. W. Nolting, S. Rex, and S. Mathi Jaya, *J. Phys.: Condens. Matter* **9**, 1301 (1997).
6. W. Nolting, G. G. Reddy, A. Ramakanth, and D. Meyer, *Phys. Rev. B* **64**, 155109 (2001).
7. C. Santos and W. Nolting, submitted to *Phys. Rev. B* (2001).
8. R. Schiller and W. Nolting, *Phys. Rev. B* **60**, 462 (1999).
9. O. K. Andersen, *Phys. Rev. B* **12**, 3060 (1975).
10. O. K. Andersen and O. Jepsen, *Phys. Rev. Lett.* **53**, 2571 (1984).
11. N. M. Mermin and H. Wagner, *Phys. Rev. Lett.* **17**, 1133 (1966).
12. A. Gelfert and W. Nolting, *phys. stat. sol. (b)* **217**, 805 (2000).
13. A. Gelfert and W. Nolting, *J. Phys.: Condens. Matter* **13**, R505 (2001).
14. H. C. Bohn, W. Zinn, B. Dorner, and A. Kollmar, *Phys. Rev. B* **22**, 5447 (1980).

15. R. Schiller, W. Müller, and W. Nolting, Phys. Rev. B **64**, 134409 (2001).
16. M. Farle, K. Baberschke, U. Stetter, A. Aspelmeier, and F. Gerhardter, Phys. Rev. B **47**, 11571 (1993).
17. R. Schiller and W. Nolting, Solid State Commun. **118**, 173 (2001).
18. R. Schiller and W. Nolting, Phys. Rev. Lett. **86**, 3847 (2001).